Nov 9th, 12:00 AM - 12:00 AM

Buckling Strength of Cold-Formed Circular Steel Column Subjected to Axial Load

Ayana Ito

Nobutaka Shimizu

Keiichi Sato

Yoshimichi Kawai

Wei-Wen Yu International Specialty Conference on Cold-Formed Steel Structures
Baltimore, Maryland, U.S.A, November 9 & 10, 2016

Buckling strength of cold-formed circular steel column subjected to axial load

Ayana ITO[1], Nobutaka SHIMIZU[1], Keiichi SATO[1] and Yoshimichi KAWAI[1]

Abstract

In this study, the global buckling behavior of a cold-formed circular steel column was discussed with a focus on the effects of its mechanical properties and initial imperfections on the behavior. As the first step, the stress–strain curves of the column under tensile and compressive loads as well as its residual stresses were investigated. Subsequently, a finite element analysis was conducted to clarify if the analysis properly simulated the stub column behavior. The analysis results obtained using measured compressive stress–strain curves and residual stresses agreed well with experimental results. Finally, another finite element analysis was performed on the long column buckling to examine the effects of its mechanical properties and initial imperfections. It was shown that the global buckling strength was affected not only by imperfections such as residual stress and out-of-straightness but also by the anisotropic mechanical properties of the material.

1. Introduction

It is well known that structural steel members have initial imperfections such as residual stress and out-of-straightness and that these imperfections affect the global buckling behavior of a member under axial compressive load. Extensive research on the global buckling behavior considering the effects of such imperfections has been conducted in the past, concluding that imperfection effects are quite significant, especially in cold-formed steel members. Reflecting

[1] Steel Structures Research Lab., Nippon Steel & Sumitomo Metal Corp., Japan

these facts, Eurocode3 (European Committee for Standardization 2005) introduced a penalty in global buckling design strength formulas for cold-formed steel members, resulting in a decrease in their design strength compared with hot-rolled steel members.

A cold-formed steel column, a type of cold-formed structural member, undergoes various cold-working processes, such as expansion, shrinkage, bending, and unbending, during the production. In addition, the member is subjected to complex loading. Strain hardening and the Bauschinger effect can induce large residual stresses, and more importantly, they may cause the material to have anisotropic mechanical properties. It is known that cold working makes a material anisotropic, which may affect its column buckling behavior by Winter (1968), Wakabayashi (1969), Kato (1978), Toma (1979), Aoki (1983) and Schmidt (1989). However, previous studies on column buckling have not paid much attention to the effects of material anisotropy. Further study on the effects of mechanical properties as well as of initial imperfections such as residual stress and out-of-straightness on column buckling is needed.

From the background mentioned above, this study aimed to quantitatively clarify the effects of anisotropic mechanical properties and initial imperfections on the global buckling strength of cold-formed steel columns. For this purpose, stress–strain curves under tensile and compressive loads and residual stress distribution were first investigated using an electric-resistance-welded (ERW) circular tube. Then, two finite element analyses were conducted. The first series intended to demonstrate whether the analyses with the measured stress–strain curves and residual stress distribution agreed with the test results. The second series was performed as a parametric study to clarify in detail the effects of material anisotropy on the global buckling strength.

2. Measurement of residual stress

2.1. Measurement method

To investigate the residual stress and its distribution of ERW circular steel tubes, an ERW tube, to which strain gauges were already attached, was cut into small coupons. The strains released by the cutting were measured using the gauges to determine the residual stresses. A JIS-STK400 steel (typical mild steel) tube having a diameter (D) of 114.3 mm and thickness (t) of 6 mm was used as the specimen. The strains were measured as follows (e.g., see Kato 1978):

i) Bi-axial strain gauges were attached at the positions shown in Fig. 1

(numbers denote measurement positions) along the circumference of the tube on both the outer and the inner faces. The steel tube member with attached gauges had a length of 230 mm. The length (L) was twice as large as the diameter (=2D).

ii) A ring-like specimen was cut from the tube, as shown in Fig. 1. The ring width was 30 mm, and strain gauges were attached along the midpoint of the width.

iii) Then, the ring-like specimen was further cut into 30 mm × 30 mm square pieces to include a pair of bi-axial strain gauges in each piece.

iv) The strains released due to the cutting were measured, and these measured values were defined as residual strains in the tube.

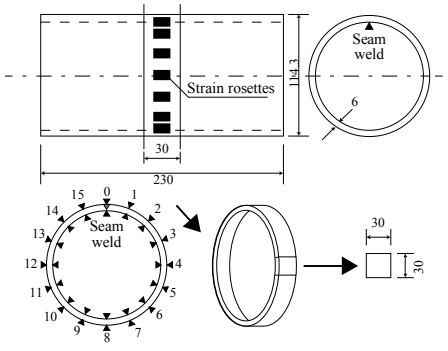

Fig. 1 Measurement of residual strains

2. 2 Measurement results

The measured residual strains are shown in Fig. 2. Note that numbers 1 and 13 are absent in the figure because the corresponding strain gauges broke when the columns were cut into pieces. The results show that the residual strains have relatively uniform distributions in both the longitudinal and the circumferential directions, except for the seam weld portion. The strains are in tension on the outer surface and in compression on the inner surface along both the longitudinal and the circumferential directions. The strains in the longitudinal direction are larger than those in the circumferential direction.

Residual stresses at the outermost edge along the thickness were calculated from these measured strains by using Hooke's law in the plane stress condition with a Young's modulus of 205,000 MPa and Poisson's ratio of 0.3, and they are shown in Fig. 3. As can be seen in the strain distributions, tension stresses act on the outer face and compression stresses act on the inner face in both the longitudinal and the circumferential directions. In addition, the residual stresses are larger in the longitudinal direction than those in the circumferential direction. As indicated later, the yield strength of the material is around 415 MPa (Table 1). Therefore, the residual stresses in the longitudinal direction reach the material yield strength. These stresses are quite high compared to the residual stresses typically assumed in cold-formed open sections.

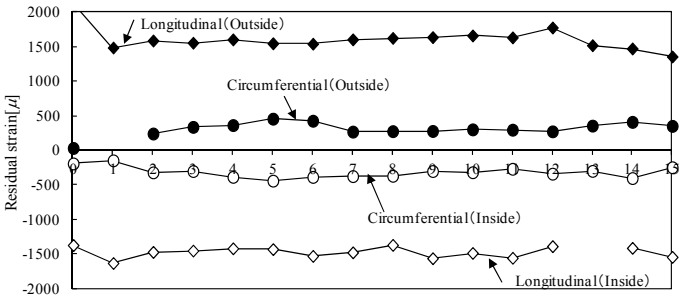

Fig. 2 Measured strains

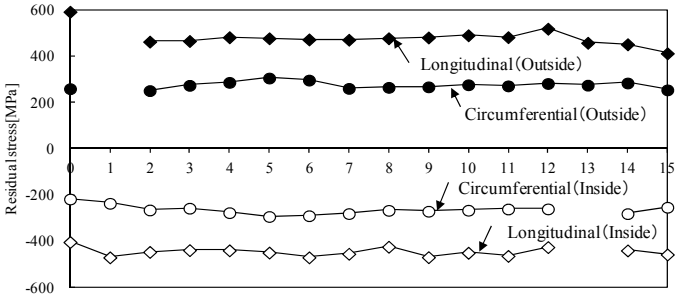

Fig. 3 Residual stresses calculated from measured strains

3. Measurement of mechanical properties

3. 1 Testing method

To obtain the stress–strain curves of the material, both tensile and compressive coupon tests were conducted as follows:

1) Tensile coupon test: The test specimen is shown in Fig. 5(a). The specimen, which had a diameter of 3 mm and gauge length of 10 mm, was sampled directly from the positions shown in Fig. 4. Specimen strains were measured by strain gauges attached to its central portion. The loading speed was assumed to be static with a strain rate of 5.0×10^{-3} s^{-1}.
2) Compressive yield test: A compressive yield test (e.g., see Tsuru 2004) was performed using the test specimen shown in Fig. 5(b), the diameter and height of which were 4.2 mm and 8.4 mm, respectively. This specimen was

also sampled from the same positions as those for the tensile test specimens. The strains of the specimen were measured by strain gauges attached to its central portion. The loading speed was the same as that in the tensile test. To prevent the end constraint, the ends of the specimen were greased with lubricating oils.

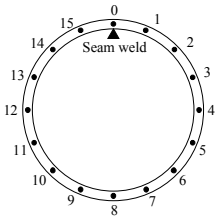

Fig. 4 Sampling locations

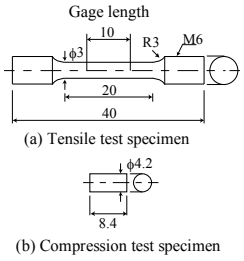

Fig. 5 Coupon test specimens

Table 1 Mechanical properties

Sampling locations	Tension			Compression	C/T
	YS $_t\sigma_y$ [MPa]	Ts $_t\sigma_u$ [MPa]	YR	YS $_c\sigma_y$ [MPa]	(YS)
0	492	553	89	434	0.88
1	416	466	89	363	0.87
2	422	471	90	355	0.84
3	414	469	88	375	0.91
4	412	471	87	355	0.86
5	415	473	88	362	0.87
6	414	472	88	343	0.83
7	411	471	87	348	0.85
8	416	468	89	357	0.86
9	411	471	87	356	0.87
10	409	471	87	346	0.85
11	410	471	87	347	0.85
12	413	471	88	349	0.85
13	416	474	88	354	0.85
14	424	476	89	355	0.84
15	427	474	90	356	0.83
average (Number 1-15)	415	471	88	355	0.85

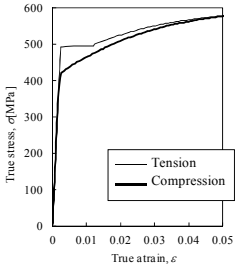

(a) Number 0

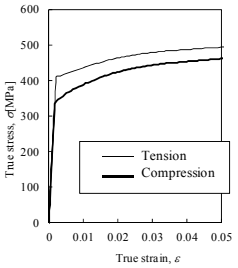

(b) Number 8

Fig. 6 True stress–strain curves

3. 2 Test results

The measured true stress–strain curves are shown in Fig. 6: (a) the number 0 denotes the seam-welded portion; (b) the number 8 denotes the side opposite to the seam-welded portion. The curves under tensile loads are higher than those under compressive loads. The mechanical properties under both tensile and compressive coupon tests are summarized in Table 1, where the yield strength was defined either as the lower yielding point when a yield plateau was observed or as the 0.2% offset value when no yield plateau was observed. The yield strength at the seam-welded portion is approximately 20% larger than that at the other portions, and this might be ascribed to the heat treatment effect through the

seam welding. Most of the yield strengths under tensile and compressive loads fall into certain ranges (i.e., tension: 409 MPa–427 MPa; compression: 343 MPa–375 MPa), excluding that of the seam-welded portion. The average ratio of the compression yield strength to the yield strength (C/T) is 0.85, meaning that the compressive values are lower than the tensile ones. This anisotropic mechanical property pertaining to yield strength can possibly be ascribed to strain hardening and the Bauschinger effect through the cold-forming processes.

4. Stub column test

4. 1 Experimental procedure

Three stub column specimens (D = 114.3 mm, t = 6 mm, and L = 342.9 mm) were tested under axial compressive loading to examine the local buckling behavior. The length of the stub columns L was three times as large as the diameter (=3D), which was short enough to restrain the interaction with global buckling.

The specimens were loaded between the top and bottom plates (500 × 500 × 20 mm) by a testing machine, and the compressive force P and longitudinal displacements δ were measured, respectively, by a load cell and displacement transducers. To have a uniform loading, both end surfaces of the specimens were mill finished, and the top and bottom plates were fixed about rotation. For securing a close contact with the plates, a hemispherical bearing was first set between the bottom plate and the head of the testing machine, and then after giving a initial loading (until P = 100 kN–200 kN), the bearing was locked with wedges. Axial load was applied statically until an apparent load decline was observed after the maximum strength.

4. 2 Test results

The load–displacement (P–δ) curves of the three stub columns are plotted in Fig. 7. After a linear behavior at the early loading stage, the P–δ curves of all specimens show gradual stiffness decrease and reach an ultimate strength determined by local buckling, as shown in Fig. 9. The P–δ curves of the three specimens agree well with each other until their maximum strengths.

The stress–strain curves derived from the stub column tests and coupon tests are plotted in Fig. 8. For the stub column tests, the stress was calculated as the ratio of the axial load P to the cross-sectional area, and the strains were determined

from the ratio of the displacement δ to the stub column length L. In the stub column tests, the tangent modulus up to the yield strength is smaller than that in the coupon tests apparently due to the residual stress. The stress–strain curves obtained in the stub column tests agree reasonably well with the compressive curves, although the tensile curves do not agree and lager than the stub column test results.

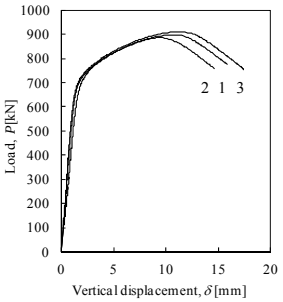

Fig. 7 Load-displacement curves

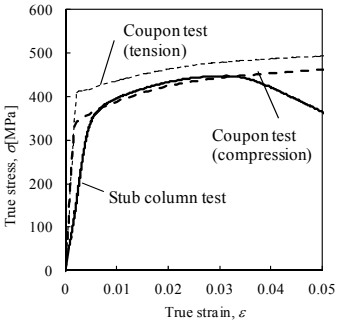

Fig. 8 Comparison of results for stub column test and coupon tests

Fig. 9 Failure mode

5. Finite element analysis of the stub column

5. 1 Analytical procedure

The buckling behavior of the stub column under compressive loads was analyzed using "MARC," a finite element analysis (FEA) program. In the analysis, the stub column specimen tested [D = 114.3 mm, t = 5.7 mm (measured thickness), L = 342.9 mm] was modeled with thick-shell elements with nine layers along the thickness.

A multi-linear stress-strain curves and the von Mises yield criterion were used in the FE models, assuming that Young's modulus and Poisson's ratio were 205,000 MPa and 0.3 respectively. Two types of stress-strain curves that were modeled based on the data obtained from the tensile and compressive coupon tests (called "tensile model" and "compressive model" hereafter) were considered in the analyses. Residual stresses were implemented into the thick-shell elements by applying those measured at the surfaces of the ring-like specimen (see Chapter 2). A linear distribution was assumed through the

thickness, and the corresponding residual stresses were introduced at the integration points in the element layers, as shown in Fig. 10(b).

As shown in Fig. 10(a), the displacements and rotations were fixed on the top and bottom faces of the FE model, except for the z direction displacements on the top face. To inhibit the sectional distortion at both ends of the model, nodes of each end were connected to each centroidal axis of the section [supporting point and loading point shown in Fig. 10(a)] with rigid links. In this model, no initial out-of-straightness was applied.

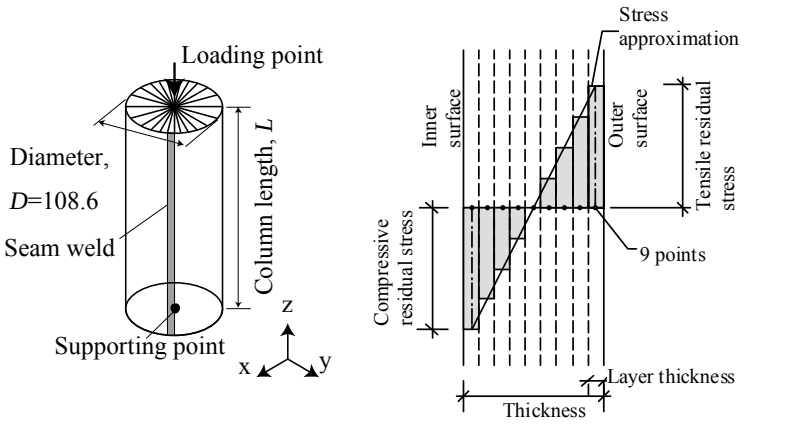

(a) FE model (b) Residual stress approximation

Fig. 10 Finite element analysis

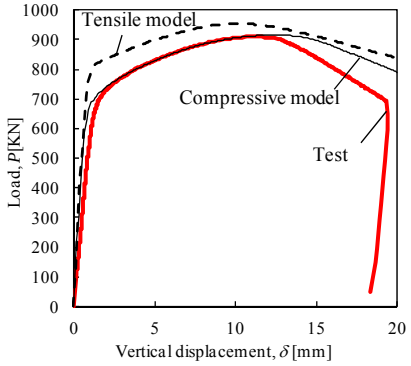

Fig. 11 Comparison of FEA and stub column test results

5. 2 Verification of the finite element model

A comparison between the FEA and test results is shown in Fig. 11. The figure shows that the results of the compressive model agree reasonably well with the test results, whereas the results of the tensile model do not fit with them. Thus, it is preferable that the FE models with compressive stress–strain curves (compressive model) be used to analyze the stub-column behavior of ERW tubes under axial compressive loads.

6. Effects of initial imperfections and anisotropic mechanical properties on global buckling strength

6. 1 Analytical procedure

The stub column FE model was expanded to a slender column FE model in order to investigate the effects of initial imperfections and anisotropic mechanical properties on the global buckling strength of ERW circular steel columns. The sectional dimensions of the steel columns were set based on the nominal values as D = 114.3 mm and t = 6 mm. In that model, the rotation around the x axis was allowed at the top and bottom ends, so that a simply supported condition at the both ends was realized. A series of finite element analyses were conducted to clarify what factors affected the buckling strengths at what degree. To do this in a rational manner, the Design of Experiment (DoE) approach (e.g., see Kempthorne 1952) was employed to make its analysis plan.

The prime factors considered here were as follows: i) residual stress in the longitudinal direction, ii) residual stress in the circumferential direction, iii) initial out-of-straightness, and iv) anisotropic mechanical properties. The effects of the above prime factors were examined for three column cases with different lengths (L = 1339, 2678, and 4016 mm; non-dimensional slenderness ratios λ_n = 0.5, 1.0, and 1.5). Two levels (upper and lower levels) were considered for each factor in making the analysis plan based on the DoE. The followings are the descriptions about the prime factors:

(1) Residual stresses

The measured residual stress distributions in the longitudinal and circumferential directions were directly applied to the analyses with two levels of maximum stress values: 200 MPa for the lower case and 400 MPa for the upper case.

(2) Initial out-of-straightness

The initial out-of-straightness was chosen as a sinusoidal initial curve with a central bow of 1/1000 and 1/5000 of the member length (L). The L/1000 was set according to Eurocode 3 (European Committee for Standardization 2005), whereas the L/5000 was chosen based on the average of the measured results (e.g., see Wakabayashi 1969).

(3) Anisotropic mechanical properties

The true stress–strain curves under tensile and compressive loads were approximated by the Swift-type equation (Swift 1952), which is expressed as follows:

$$\sigma = C\left(\varepsilon_0 + \varepsilon^p\right)^n \qquad (1)$$

where C, ε_0, and n are the material constants, which can be identified by comparison with experimental data. The constants obtained based on the least-squares method are listed in Table 2. The approximated stress–strain curves agree with the test results, as shown Fig. 12. For applying the DoE, two levels were set using the n value: 0.08 for the lower case and 0.10 for the upper case.

Table 3 shows the prime factors considered and the two levels set in this analysis. Assuming that the four prime factors are independent each other, an orthogonal array of L_8 (2^7) was used for importance evaluation among the factors. Eight combinations of the factors were allotted, as summarized in Table 4. The array was applied to three column length cases (λ_n = 0.5, 1.0, and 1.5); therefore, in total, 24 finite element models were executed.

Table 2 Swift equations

	C	$\varepsilon 0$	n
Tension	634	0.0017	0.08
Compression	634	0.0017	0.10

Table 3 Factors

Factor	1	2
Circumferential residual stress[MPa]	200	400
Longitudinal residual stress[MPa]	200	400
Initial out of straightness[mm]	L/5000	L/1000
Mechanical property, n value	0.08	0.10

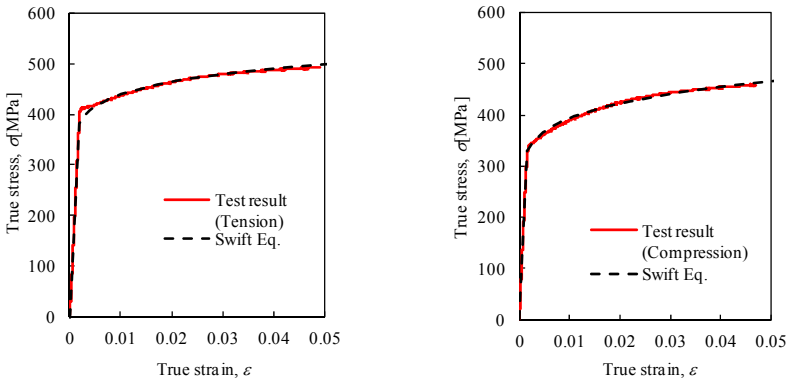

(a) Tension (b) Compression

Fig. 12 Comparison of Swift equations with test results

Table 4 L8 Orthogonal array

	Residual stress[MPa]		Initial out-of-straightness [mm]	Mechanical property, (n value)
	Circumferential	Longitudinal		
No.1	200	200	L/5000	0.08
No.2	200	200	L/1000	0.08
No.3	200	400	L/5000	0.10
No.4	200	400	L/1000	0.10
No.5	400	200	L/5000	0.10
No.6	400	200	L/1000	0.10
No.7	400	400	L/5000	0.08
No.8	400	400	L/1000	0.08

Table 5 FEA results

	Maximum strengh of slender columns[kN]		
	λ_n=0.5	λ_n=1	λ_n=1.5
No.1	758	625	365
No.2	733	562	330
No.3	668	493	299
No.4	642	451	271
No.5	642	532	341
No.6	624	474	305
No.7	737	570	327
No.8	714	510	300

6. 2 Analysis results

The maximum strengths obtained from the FEA results of the slender columns are listed in Table 5. The results were then analyzed using Analysis of Variance (ANOVA) (e.g., see Kempthorne 1952), which is a statistical analysis technique that helps reduce the error variance and quantifies the dominance of factors. Table 6 presents the ANOVA tables for each column length case (λ_n = 0.5, 1.0, and 1.5).

In the case of λ_n = 0.5 [Table 6(a)], the mechanical properties have the highest contribution of 89.5%, followed by initial out-of-straightness (5.6%), and residual stress along the circumferential direction (4.7%). The contribution of the residual stress along the longitudinal direction is zero in this case.

Table 6 ANOVA table for responses

(a) λ_n=0.5

Factor	Degree of freedom	Sum of squares	Variance	F value	Contribution ratio
Circumferential residual stress	1	882	882	139	4.7%
Longitudinal residual stress	1	2	2	0	0.0%
Mechanical property, n value	1	16745	16745	2644	89.5%
Initial out of straightness	1	1058	1058	167	5.6%
Error term	3	19	6	-	0.2%
Total	7	18706	18693	2951	100.0%

(b) λ_n=1.0

Factor	Degree of freedom	Sum of squares	Variance	F value	Contribution ratio
Circumferential residual stress	1	253	253	6	0.9%
Longitudinal residual stress	1	3570	3570	81	15.5%
Mechanical property, n value	1	12561	12561	285	55.1%
Initial out of straightness	1	6216	6216	141	27.2%
Error term	3	132	44	-	1.4%
Total	7	22733	22645	512	100.0%

(c) λ_n=1.5

Factor	Degree of freedom	Sum of squares	Variance	F value	Contribution ratio
Circumferential residual stress	1	8	8	1	0.0%
Longitudinal residual stress	1	2592	2592	239	42.9%
Mechanical property, n value	1	1405	1405	130	23.1%
Initial out of straightness	1	1985	1985	183	32.8%
Error term	3	33	11	-	1.2%
Total	7	6022	6000	553	100.0%

In the case of λ_n = 1.0 [Table 6(b)], the mechanical properties have the highest contribution (55.1%), followed by initial out-of-straightness (27.2%), residual stress along the longitudinal direction (15.5%), and residual stress along the circumferential direction (0.9%).

In the case of λ_n = 1.5 [Table 6(c)], the residual stress in the longitudinal direction has the most significant effect (42.9%), while mechanical properties (23.1%) and initial out-of-straightness (32.8%) have lesser influence. The contribution of the residual stress in the circumferential direction is zero for this slenderness ratio.

According to the relationship between the contributions obtained from the ANOVA and the non-dimensional slenderness ratio (λ_n), which is shown in Fig. 13, the contribution ratios depend on the non-dimensional slenderness ratio. For

small slenderness ratios (λ_n = 0.5 and 1.0), the mechanical properties affect buckling strength more than the initial imperfections. In contrast, for large slenderness ratios (λ_n = 1.5), the contributions of the mechanical properties and imperfections (residual stress in the longitudinal direction and initial out-of-straightness) are relatively comparable. Hence, the mechanical properties obviously become a significant factor for plastic buckling, whereas the residual stress and the initial out-of-straightness greatly influence elastic buckling.

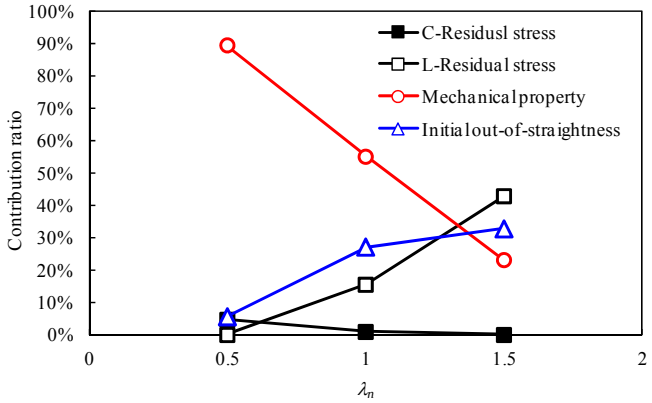

Fig. 13 Effects of imperfections and anisotropic mechanical properties

7. Conclusion

This study was conducted to clarify the effects of anisotropic mechanical properties and initial imperfections on the global buckling strength of cold-formed steel columns (ERW tubes) in a quantitative manner. Based on the results, the following conclusions were drawn:

(1) The residual stress distributions and the stress–strain curves of the ERW tubes were investigated. The measured results confirmed that the ERW tube had large residual stresses and anisotropic mechanical properties. It was anticipated that the anisotropic mechanical properties were caused by strain hardening and the Bauschinger effect during the cold-forming processes.

(2) FEA of a stub column of an ERW tube was described and performed in this study. A method for building the models considering the residual stresses and the compressive stress–strain curves was presented. The numerical predictions agreed reasonably well with the experimental load-deformation curves.

(3) The DoE approach and the ANOVA method were used to investigate the contribution of each parameter on the global buckling strength of ERW tubes.

It was found that the anisotropic mechanical properties affected the strength most, followed by the initial out-of-straightness and the residual stresses for small slenderness ratio cases. For large slenderness ratio cases, the residual stress along the longitudinal direction and the initial out-of-straightness were major affecting factors.

Through this study, it was shown overall that the global buckling strength was affected not only by imperfections, such as residual stress and out-of-straightness, but also by the anisotropic mechanical properties of the material.

References

Aoki, T., Fukumoto, Y. (1983). "Strength distribution of centrally compressed cold-formed-welded steel tubular columns with small diameter.'' Proceedings of Japan Society of Civil Engineers, (337) 17-26 (in Japanese)

European Committee for Standardization (2005) "Eurocode3-Design of steel structures''

Kato, B., Aoki, H. (1978). "Residual stresses in cold-formed tubes." J. Strain Anal., 13 (4) 193-204

Kempthorne, O. (1952). "The Design and Analysis of Experiments''

Schmidt, L. C., Morgan, P. R. (1989). "The influence on steel tubular strut load capacity of strain hardening, strain aging and the bauschinger effect." J. Construct. Steel Research 14, 107-119

Swift, H. W. (1952). "Plastic instability under plane stress.'' Journal of the Mechanics and Physics of Solids, 1 1-18

Toma, S., Chen, W. F. (1979). "Analysis of fabricated tubular columns.'' ASCE, 105, 2343-2366

Tsuru, E., Asahi, H. (2004). "Collapse pressure prediction and measurement methodology of UOE pipe.'' International Journal of Offshore and Polar Engineering, 14

Wakabayashi, M., Nonaka, T. and Nishikawa, K. (1969). "An experimental study on the buckling of circular welded tubes.'' Disaster Prevention Research Institute Annals, Kyoto University, (12A) 439-462 (in Japanese)

Winter, G., Uribe, J. (1968). "Effects of cold work on cold-formed steel members." in Thin-Walled Steel Structures, Gordon and Breach Science Publishers, New York